Multiple mechanisms mediate enhanced immunity generated by mAb-inactivated *F. tularensis* immunogen

Bibiana V. Iglesias[1], **Constantine Bitsaktsis**[2], **Giang Pham**, **James R. Drake**, **Karsten R.O. Hazlett**, **Kristen Porter**, and **Edmund J. Gosselin**[*]

Center for Immunology and Microbial Disease, Albany Medical College, Albany, NY 12208

Abstract

We have previously demonstrated that immunization with inactivated *Francisella tularensis*, a Category A intracellular mucosal pathogen, combined with IgG2a anti-*F. tularensis* monoclonal antibody, enhances protection against subsequent *F. tularensis* challenge. To understand the mechanism(s) involved, we examined the binding, internalization, presentation, and *in vivo* trafficking of inactivated *F. tularensis* in the presence and absence of opsonizing monoclonal antibody. We found that when inactivated *F. tularensis* is combined with anti-*F. tularensis* monoclonal antibody, presentation to *F. tularensis*-specific T cells is enhanced, this enhancement is Fc receptor-dependent, and requires a physical linkage between the monoclonal antibody and the inactivated *F. tularensis* immunogen. This enhanced presentation is due, in part, to enhanced binding and internalization of inactivated *F. tularensis* by antigen presenting cells, and involves interactions with multiple Fc receptor types. Furthermore, targeting inactivated *F. tularensis* to Fc receptors enhances dendritic cell maturation and extends the time period over which antigen presenting cells stimulate T cells. *In vivo* trafficking studies reveal enhanced transport of inactivated *F. tularensis* immunogen to the Nasal Associated Lymphoid Tissue in the presence of monoclonal antibody, which is FcRn-dependent. In summary, these are the first comprehensive studies using a single vaccine protection model/immunogen to establish the array of mechanisms involved in enhanced immunity/protection mediated by an Fc receptor-targeted mucosal immunogen. These results demonstrate that multiple cellular/immune mechanisms contribute to Fc receptor-enhanced immunity.

Keywords

Fc receptors; Vaccine; Mucosal; *F. tularensis*; Antigen presentation; Trafficking

[*]Corresponding author: Mailing address: Center for Immunology and Microbial Disease, MC-151, Albany Medical College, 47 New Scotland Avenue, Albany, NY 12208. Phone: 518-262-5562. FAX: 518-262-6161. gossele@mail.amc.edu.
[1]Currently: Regeneron Pharmaceuticals, 777 Old Saw Mill River Road, Tarrytown, NY 10591
[2]Currently: Department of Biological Sciences, Seton Hall University, South Orange, NJ 07079

Introduction

Francisella tularensis (*Ft*) is a Category A mucosal pathogen that represents a significant bioterror threat [1]. We have previously demonstrated that intranasal (i.n.) administration of immune complexes (ICs) composed of inactivated *Ft* (i*Ft*) and IgG2a monoclonal antibody (mAb) specific for i*Ft* LPS, in which free/non-i*Ft* bound mAb has been removed (mAb-i*Ft* ICs), enhances the immune response to, and protection against *Ft* challenge [2]. We further demonstrated that the enhanced protection observed was Fc receptor (FcR)-dependent. In addition, this was the first study to demonstrate that targeting an immunogen to FcR i.n. enhances protection against a mucosal infectious disease challenge. Subsequent studies have verified the potential for using FcR-targeted immunogens as effective mucosal vaccines [3–6].

While numerous mechanisms, including enhanced Ag presentation, have been predicted to be involved in FcR-enhanced immune responses, comprehensive studies using a proven FcR-targeted mucosal vaccine strategy to actually define these specific mechanisms have not been conducted [7–10]. Some of the proposed mechanisms involved include the following: It has been proposed that complement-mediated binding of antibody (Ab)-Ag ICs to APCs, not FcR binding, may be responsible for Ab-Ag IC-mediated immune enhancement. However, this has been contradicted in studies using FcR knockout (KO) mice, in which FcR were required for immune enhancement [9]. Alternatively, up regulation of MHC class II and second signal molecules, as a result of FcR cross-linking on APCs, could also lead to enhanced Ag presentation. However, in previous *in vitro* studies using human IgG-Ag ICs and monocytes as APCs, we did not observe increased expression of these molecules as a consequence of IC-FcR interaction [11]. Studies using dendritic cells (DCs) however, have indicated that Ab-Ag ICs can induce DC maturation [12], although this was later contradicted by a study suggesting IC interaction with the inhibitory FcR (FcγRIIB) blocks DC maturation induced by ICs [13]. In addition, as previously indicated above, more efficient Ag-binding and internalization is believed to play an important role in IC-enhanced immune responses. However, this is dependent on not only the concentration of ligand, but the valency of the ligand, the number of FcR expressed on the APC surface, and whether or not the particular FcγR is occupied with serum IgG [9, 14]. In the latter case, the amount of FcR cross-linking required to induce internalization appears to actually be reduced when FcγRI is occupied [9, 14]. Engaging FcR on APCs can also induce cytokine production [15–17]. The cytokine milieu can then determine the type and degree of the immune response. For example, studies, in which the activating FcγRIIA on monocyte-derived DCs was ligated, resulted in secretion of IL-10 and IL-6 (stimulates B cells and plasma cells), and TNF alpha and IL-8 (chemoattractants). However, the cytokines produced can vary with the source of DCs and the ratio of activating and inhibitory (FcγRIIB) receptors engaged [12, 18]. Furthermore, the impact of Ag targeting to FcR on Ag persistence, which is observed when Ag is targeted to the B cell receptor [19], or Ag trafficking to lymphoid tissues *in vivo* [8, 9], remains unclear. More recently, and contrary to prior belief, studies have clearly demonstrated the neonatal Fc receptor (FcRn), which binds IgG Fc, is present in the epithelium of the nasal mucosa in adult mice [4], and that targeting Ags to FcRn via this route also enhances the immune responses to, and protection against, mucosal pathogens [4, 5]. This is also consistent with our previous studies indicating the presence of FcRn is critical for the

enhanced protection that we observe when utilizing mAb-i*Ft* ICs as protective mucosal immunogen [2].

Thus, we sought to clarify the mechanism(s) involved in FcR-enhanced immunity, including the specific role of FcRn, by conducting a comprehensive analysis of the numerous potential mechanisms involved in FcR-targeted vaccination using a single FcR-targeted model immunogen, which has been proven to be effective in not only enhancing the immune response *in vivo*, but also producing protection against subsequent infectious disease challenge.

Results

Enhanced Protection Against Ft Challenge Following i.n. Administration of mAb + iFt ICs

We have previously demonstrated that mAb-i*Ft* ICs from which free/unbound mAb has been removed via centrifugation, when administered i.n., enhance protection against subsequent i.n. challenge with *Ft* [2]. Furthermore, enhanced protection was not observed when administering either mAb alone or F(ab′)$_2$ mAb-i*Ft* ICs [2]. To facilitate the conduct of these specific studies, as well as future use of this approach as a vaccine strategy, we first determined whether anti-i*Ft* mAb ± i*Ft* ICs, in which free/unbound anti-i*Ft* mAb is not removed (mAb + iFt ICs), could be used in place of mAb-i*Ft* ICs (free/unbound mAb removed) [2]. In figure 1A Western Blot was utilized to verify the formation of ICs following incubation of anti-i*Ft* mAb with i*Ft*. To accomplish this using Western Blot, it was necessary to remove free/unbound mAb, as was done in our previously published studies. Importantly, the incubation steps prior to centrifugation were the same in both our published studies in which free mAb was removed (mAb-i*Ft* ICs) and the present study in which free mAb is not removed (mAb + i*Ft* ICs). Thus, the ICs detected in Fig. 1A reflect ICs formed regardless of whether free/unbound mAb is or is not removed. Most importantly, the sole purpose of this experiment was to verify IC formation. In fact, ICs were formed and there was a significant increase in IC formation in the presence of 5 μg versus 1μg of mAb (Fig. 1A). We then immunized and boosted mice i.n. with these mixtures and challenged 14 days later i.n. with either *Ft* LVS (Fig. 1B) or *Ft* SchuS4 (Fig. 1C). Similar to studies using mAb-i*Ft* ICs (free/unbound mAb removed) [2], a significant enhancement of protection against both strains of *Ft* was observed with mAb + i*Ft* ICs (free/unbound mAb present). Also, consistent with previous studies using mAb-i*Ft* ICs, while mAb + i*Ft* ICs made with 1 μg mAb were sufficient to protect against *Ft* LVS challenge, mAb + i*Ft* ICs made with 5 μgs mAb were required to protect against *Ft* SchuS4 challenge. Thus, use of mAb + iFt ICs represents a relatively simple and straightforward approach for targeting immunogens to FcR. This is particularly the case in those instances where a protective Ag cannot be identified and the use of inactivated organisms is required, such as is currently the case with *Ft*.

Enhanced T cell Responses in the Presence of Ft-Specific mAb

One of the mechanisms by which mAb + i*Ft* ICs may enhance immune responses *in vivo* is through the induction of enhanced T cell activation. Thus, we examined the response of an *Ft*-specific T cell hybridoma (FT256D10) to APCs incubated with either i*Ft* alone or a mAb + i*Ft* ICs. The T cells were incubated with Peritoneal Exudate Cells (PECs)/Macrophages

(MØ) obtained from Balb/c mice, which are histocompatible with the T cell hybridoma, and either i*Ft* or anti-i*Ft* mAb + i*Ft* ICs. After 24 hours, the supernatant was collected and IL-5 levels (a marker of the T cell response) were measured (Fig. 2). We observed that the level of IL-5 in supernatants from T cells and APCs incubated with mAb + i*Ft* ICs was significantly higher than in the supernatants of T cells and APCs incubated with i*Ft* alone (Fig. 2) and that the enhancement was both mAb (Fig. 2A) and i*Ft* (Fig. 2B) concentration dependent. Alternatively put, mAb in the absence of sufficient amounts of Ag did not enhance T cell activation, indicating mAb alone does not stimulate the enhanced T cell activation observed when both mAb + i*Ft* ICs are present. Furthermore, enhancement was eliminated if the i*Ft*-specific mAb was replaced with a non-specific isotype (Ig2a) control mAb (Fig. 2C), or if the Fc portion of the i*Ft*-specific mAb was removed (Fig. 2D). Thus, enhanced presentation of i*Ft* is one mechanism by which mAb + i*Ft* ICs can exert their effect on the immune response, and this effect is Fc-dependent.

Anti-iFt mAb Mediates Enhanced iFt Binding to APC

One factor that can contribute to enhanced processing and presentation of i*Ft* by APCs, is increased binding of i*Ft* to APCs in the presence of mAb. We thus tested whether in the presence of mAb-i*Ft* there is increased i*Ft* binding to APCs via FcR, as compared to i*Ft* alone. To demonstrate visually, enhanced binding of mAb + i*Ft* ICs versus i*Ft* alone to FcR, FcR-bearing MØs were incubated with media, i*Ft*, or mAb + i*Ft* ICs at 4°C and unbound i*Ft* removed. In fact, we observed a significant increase in the number of bound bacteria in the presence of anti-i*Ft* mAb + i*Ft* ICs versus i*Ft* alone (Figs. 3A–D). This increase was dependent on both mAb (Fig. 3E) and i*Ft* (Fig. 3F) concentration. Furthermore, approximately 50% of the mAb-mediated i*Ft* binding could be blocked with monomeric IgG2a (Fig. 3G). Monomeric IgG2a primarily blocks the high affinity FcγRI. The mAb 2.4G2, which blocks FcγRII and FcγRIII, blocked approximately 70% of the mAb-i*Ft* binding (Fig. 3H). When combining monomeric IgG2a with mAb 2.4G2, nearly 100% of mAb-mediated i*Ft* binding was eliminated (Fig. 3I). Thus, enhanced binding of i*Ft* to APCs in the form of mAb + i*Ft* ICs represents another contributing mechanism by which mAb + i*Ft* ICs impact the immune response via FcR-enhanced delivery of Ag to APCs.

A Physical Linkage Between mAb and Ag is Required for FcR-Mediated Enhancement of Ag Presentation by APCs

We also considered the possibility that the impact of mAb + i*Ft* ICs on the presentation of i*Ft* was not dependent on i*Ft* being directly targeted to FcγR, but rather due to signaling events initiated by cross-linking FcγR. Thus, we determined whether mAb-i*Ft* added to APCs could enhance the presentation of an Ag other than i*Ft*, specifically Hen Egg Lysozyme (HEL). In this case, an HEL-specific T cell hybridoma (LY50.5) was cultured in the presence of APCs and increasing concentrations of HEL containing either media, i*Ft*, mAb-i*Ft*, or mAb alone. After 24 hours, supernatant was collected and IL-5 levels were measured. As shown in Fig. 4, the presence of mAb-i*Ft* did not impact the level of IL-5 produced by the T cell hybridoma in response to HEL, regardless of whether media, i*Ft*, mAb-i*Ft*, or mAb alone was present (Fig, 4A). The latter was not due to a failure of the mAb-i*Ft* to mediate enhanced presentation of i*Ft* (Fig. 4B). Furthermore, when HEL-

specific mAb was bound to HEL, HEL presentation was enhanced (Fig. 4C), as was the presentation of HEL when i*Ft* was chemically labeled with HEL and anti-i*Ft* mAb bound (Fig. 4D). Finally, consistent with the inability of mAb-i*Ft* to stimulate enhanced presentation of HEL, neither MHC class II expression or expression of second signal molecules on these APCs, were enhanced in the presence of mAb-i*Ft* (data not shown). Thus, cross-linking FcR with mAb + i*Ft* ICs alone is insufficient to enhance Ag presentation by APCs. Rather, a direct linkage between the Ag being presented and the mAb is required.

The Rate of iFt Internalization is Increased in the Presence of Anti-iFt mAb

Another mechanism by which i*Ft* processing and presentation could be enhanced, is via an increased rate of i*Ft* internalization by APCs. To address this possibility, the amount of i*Ft* internalized by APCs was analyzed utilizing flow cytometry. Cells were pulsed for one hour with 200 i*Ft* organisms/APC at 4°C on a rocker. Cells were then washed and incubated at 37°C for varying periods of time. Once the incubation was complete, the cells were cooled immediately on ice, washed, and incubated with pronase in order to remove the non-internalized i*Ft*. Once the non-internalized i*Ft* was removed from the surface of the cells, they were washed again and fixed. The mean fluorescence intensity (MFI) was then determined for each time point. As shown in Fig. 5, it took approximately 3–4 hours for internalization to be detected in the form of increased fluorescence of pronase-stripped cells, when pulsing with i*Ft* alone (Fig. 5A). However, the increase was much stronger and more rapid when anti-i*Ft* mAb was present, occurring in five minutes or less (Fig. 5B). Importantly, the rate of internalization for i*Ft* alone remained similar even when the number of organisms/APC was increased by 10 fold. (Fig. 4C). Thus, not only is i*Ft* binding to APCs enhanced in the presence of i*Ft*-specific mAb, but also the rate of i*Ft* internalization by APCs.

Enhanced Presentation of iFt Persists in the Presence of anti-iFt mAb

Since we observed an increased T cell response, increased binding, and more rapid internalization of the i*Ft* in the presence of anti-i*Ft* mAb, we wanted to know how these changes impact the kinetics of Ag processing and presentation. To examine this, APCs were allowed to take up and process i*Ft* in the presence and absence of mAb for 0, 1, 2, 4, 8, 22 and 26 hours. Following each incubation time point, APCs were fixed and incubated with T cells as a read out of i*Ft* processing. After 24 hours of APC plus T cell culture, the supernatant was collected and IL 5 was measured. As early as 4 hrs after i*Ft* pulse, the T cell response in the presence of mAb was increased above that of i*Ft* alone (Figs. 6A). Furthermore, the length of time processed i*Ft* was available on the surface of the APCs for presentation was also increased (Figs. 6A). To further investigate the latter observation, APCs were allowed to internalize and process the Ag for 8 hours, then the non-bound/non-internalized Ag was washed away and the cells were either fixed immediately or fixed after 15, 18, 21 or 36 hours of additional incubation. As demonstrated in Figure 6B, when i*Ft* is internalized in the presence of anti-i*Ft* mAb, up to 36 hours after free Ag is removed, an enhanced response by T cells to processed i*Ft* is observed, as compared to APCs pulsed with i*Ft* alone. Thus, the enhanced i*Ft* presentation induced by mAb-i*Ft* begins as soon as 4 hours post i*Ft* addition and also persists up to 36 hours after the i*Ft* pulse.

Enhanced iFt Binding, Presentation, and iFt Persistence is Also Observed With DCs in the Presence of mAb + iFt ICs

Since all the studies up to this point had focused on PECs/MØs as APCs, we wanted to know whether mAb + i*Ft* ICs would have a similar impact on DCs. Interestingly, the level of enhanced binding (Fig. 7A) and enhanced presentation (Fig. 7B) was even more dramatic when using DCs as APCs. In addition, in contrast to MØs, the expression of MHC class II and second signal molecules (DC maturation markers) was increased in the presence of mAb-i*Ft* versus i*Ft* (Fig. 7C). However, i*Ft* alone also induced a significant increase in the expression of these markers (Fig. 7C). Furthermore, the higher levels of i*Ft* presentation by DCs, induced in the presence of mAb-i*Ft*, also demonstrated similar persistence to that of MØs (Figs. 6 and 7D). Thus, with the exception of MHC class II, CD80, and CD86 expression, which is enhanced by mAb + i*Ft* ICs on DCs, but not on MØs (data not shown), the impact of mAb + i*Ft* ICs on i*Ft* binding, presentation, and Ag persistence, is similar to that of MØs.

Enhanced Localization of iFt to NALT in vivo

It had been previously hypothesized that one potential impact of targeting Ag to Fc receptors *in vivo* may be to enhance Ag trafficking to lymphoid organs. Given that our immunizations are i.n., we wanted to test this hypothesis with regards to Nasal Associated Lymphoid Tissue (NALT). Utilizing qPCR to detect i*Ft* localization after i.n. administration of i*Ft* and mAb-i*Ft*, we observed nearly a 10 fold increase in the amount of i*Ft* trafficking to the NALT by 30 minutes post-administration of mAb-i*Ft*, as compared to i*Ft* alone (Fig. 8A). Furthermore, prior indications that FcRn can play a significant role in Ag transport across the epithelium in adults [4, 5, 8, 20–23], was confirmed in the case of mAb + i*Ft* ICs (Fig. 8B). Specifically, when using FcRn KO mice in similar trafficking studies, the enhanced trafficking of mAb-i*Ft* observed with WT mice (Fig. 8A) was eliminated (Fig. 8B). Thus, another mechanism by which mAb + i*Ft* ICs exert their effect on the immune response is via enhanced transport of i*Ft* to the NALT via FcRn.

Discussion

Numerous studies have demonstrated that targeting Ag to FcR can enhance the immune response to Ag [12, 24–28]. In 2008, we demonstrated for the first time, that targeting Ag to FcR i.n. could also enhance protection against a subsequent challenge with the highly virulent mucosal pathogen *Ft* [2]. Utilizing this model, we now provide the first comprehensive study examining the potential mechanism(s) that contribute to this immune enhancement.

Numerous studies have suggested one mechanism of immune enhancement involves enhanced presentation of the FcR-targeted immunogen [17, 21], which is generally believed to be the primary contributor. However, a comprehensive study using an established FcR-targeted protective immunogen, such as mAb-i*Ft*, has not been conducted to determine if this is in fact the case. In this study, we verify that FcR-dependent enhanced presentation is a significant component of the enhanced response to FcR targeted i*Ft* (Fig. 2), and that targeting of i*Ft* to FcR on APCs enhances both i*Ft* binding and internalization (Figs. 3 and

5). We also demonstrate that the observed FcR-mediated enhancement in i*Ft* presentation requires a physical linkage between i*Ft* and the mAb that engages the FcR (Figs. 4A–D). In other words, simply cross-linking FcR is not sufficient to enhance Ag presentation. This is consistent with the idea that enhanced Ag binding and Ag internalization is critical to the enhanced presentation observed. The fact that cross-linking MØ FcR with mAb-i*Ft* did not enhance expression of MHC class II or second signal molecules (data not shown) is also consistent with this observation and previous observations by this laboratory in which similar results were obtained using human IgG-Ag ICs and human monocytes [11]. However, the impact of ICs on DC maturation is more controversial. While some studies have indicated that DC maturation can be enhanced in the presence of ICs [12], more recent studies have suggested ICs inhibit DC maturation via engagement of FcγRIIB, the inhibitory FcR [13]. In fact, despite the failure of mAb + i*Ft* ICs to enhance MHC class II and second signal molecule expression on MØs, DC maturation (indicated by upregulation of both MHC class II and second signal molecules), was enhanced in the presence of mAb + i*Ft* ICs (Fig. 7C). The latter is likely explained by differences between these and other published studies, and the numerous variables involved. Specifically, the study, which demonstrates inhibition, utilized ICs composed of OVA and rabbit anti-OVA IgG, combined with human monocyte-derived DCs, as apposed to our studies, which utilized ICs composed of mouse IgG2a mAb + i*Ft* ICs and mouse DCs. In this regard, the size of the ICs, the valency, and differences in inter- and cross-species binding of IgG isotypes to FcR, all significantly impact, which FcR (activating versus inhibitory) are engaged [8, 9, 12, 17]. It is likely in our case, engagement and activation of the stimulatory FcRs dominates that of the inhibitory FcR, resulting in the enhanced DC maturation we observe.

This paper also demonstrates for the first time that targeting Ag to FcR results in Ag presentation persisting at higher levels for an extended period of time (Figs. 6 and 7). As with enhanced Ag binding and presentation, this was observed for both MØs and DCs (Figs. 6 and 7). In fact, a similar observation has been made when targeting Ag to the B cell Ag receptor [19]. Thus, this may represent a common mechanism used by many APCs to enhance and prolong the immune response, and thus immune protection. Importantly, despite the fact mAb + i*Ft* ICs enhance T cell activation, we have not observed any physical side effects following immunization with ICs, whether or not free mAb is present. Histological analysis of lung tissues and BAL 1, 3, and 6 days post immunization also show no significant differences in cellular infiltration (nearly absent) between PBS, i*Ft*, or mAb + i*Ft* IC-immunized mice (Data not shown). Never the less, it is likely that the inflammatory response is enhanced within the NALT following administration of ICs, as reflected in the resultant enhanced humoral and cellular immune responses.

It has also been proposed that an additional mechanism by which FcR-targeted immunogens enhance the immune response is by facilitating the trafficking of Ag to lymphoid tissues [9]. In the case of mAb-i*Ft* this does hold true, in that i*Ft* transport to the NALT was enhanced in the presence of anti-i*Ft* mAb and was FcRn-dependent. (Fig. 8B). In fact, since our original publication in 2008 [2], other laboratories have published papers demonstrating that targeting Ag to FcR i.n. can enhance the protective response to other pathogens, and that this can be accomplished by targeting Ag specifically to FcRn [3–5]. FcRn is not only expressed in

the nasal epithelium, but can also mediate the transport of Ag/immunogen across epithelial barriers to the underlying lymphoid tissues in adults [20, 22, 23]. Furthermore, in our 2008 study, enhanced protection following i.n. immunization with mAb-i*Ft* was lost in FcRn KO mice, suggesting FcRn was playing a key role [2]. Thus, our data support the hypothesis that mAb + i*Ft* ICs first engage FcRn for transepithelial transport to the NALT, followed by engagement of FcγR on APCs within the NALT. However, further trafficking studies will be needed to specifically verify this hypothesis. It should also be noted Ags can also be transported by M cells [29], which may also play a role. In fact, in regard to the latter, we have recently published studies in which engagement of FcRn cannot occur, but never the less enhanced mucosal immunity is still observed when targeting the immunogen to FcγRI on mucosal APCs [6].

In summary, utilizing a proven FcR-targeted protective mucosal immunogen [2], we demonstrate that a number of mechanisms contribute to the enhanced immunity and protection observed when targeting an immunogen to FcR. Specifically, FcR targeting mediates enhanced Ag binding, as well as more rapid Ag internalization, leading to enhanced activation of Ag-specific T cells. Consistent with this, Ag must be physically attached to the FcR-targeting component (in this case mAb) to observe enhanced presentation. In addition, not only is the T cell response enhanced, but also that enhancement is maintained over an extended period of time. Furthermore, DC maturation is also enhanced, as well as the FcRn-mediated trafficking of i*Ft* to NALT. Thus, the impact of targeting Ag to FcR is multi-pronged with each mechanism involved having the potential to significantly contribute to enhanced immunity and protection. By understanding and further optimizing each of these events, one has the potential to further improve on FcR targeting as an effective mucosal vaccine platform. Furthermore, the fact that mAb + i*Ft* ICs are as effective as mAb-i*Ft* ICs in which free mAb has been removed [[2] and Fig. 1] will further facilitate the application of this specific strategy in a clinical setting.

Materials and Methods

Reagents

The Ag HEL and Pronase were purchased from Sigma (St. Louis, MO). Endotoxins were removed from HEL using Detoxi-Gel from Pierce (Rockford, IL). Cell-Tak was purchased from BD Biosciences (San Diego, CA) and used as directed by the vendor. Cholera Toxin Subunit B (recombinant)-Alexa Fluor 647 conjugate was purchased from Invitrogen (Carlsbad, CA). The mouse IgG2a anti-*Ft* LPS mAb used to make mAb + i*Ft* ICs, was purchased from Fitzgerald (cat # 10-F02, clone# M0232621, Acton, MA). F(ab′)$_2$ mAb against *Ft* LPS was prepared using an F(ab′)$_2$ preparation kit from Pierce according to vendor instructions. Anti-mouse F4/80 Ab was purchased from Invitrogen. Anti-mouse CD16/32 (2.4G2) F(ab′)$_2$ Ab was purchased from BD Biosciences. Anti-mouse MHC class II (I-A/I-E), CD83 and DEC205 Ab were purchased from eBioscience (San Diego, CA). Anti-mouse CD80 and CD86 Ab were purchased from BioLegend (San Diego, CA). IgG2a isotype control Ab was purchased from MP Biomedicals, LLC (Solon, OH). All other isotype control Abs were purchased from BioLegend.

Cells

Either PEC/MØs or DCs were used as APCs in these studies. PEC/MØs were obtained from Balb/c or C3H/HeN mice. DCs were derived from Balb/c bone marrow cells and cultured for one week in the media described below supplemented with 50 ng/ml of FLT3 (R&D Systems, Minneapolis, MN). The *Ft*-specific T cell hybridoma (FT256D10) is specific for an *Ft* ribosomal protein-derived peptide, and was provided by Dr. Jeffrey Frelinger (University of North Carolina at Chapel Hill). The hybridoma was cultured in RPMI 1640 (CellGro, Manassas, VA) containing 10% FBS (HyClone, Logan, UT), 2mM L-Glutamine (CellGro), MEM non essential aminoacids (CellGro), 1 mM Sodium Pyruvate, 50 μM 2-ME, 100 U/ml Penicillin, 100 μg/ml Streptomicin (Gibco), and 500 μg/ml of Hygromycin B (CellGro). The HEL-specific T cell hybridoma (Ly50.5) and Balb/c bone marrow-derived DCs were cultured in the same media without the addition of Hygromycin.

Mice

Balb/c, C57BL/6, and C3H/HeN mice were purchased from Taconic Laboratories (Hudson, NY). All mice were housed at the Animal Resources Facility at Albany Medical College. The mice were used at 6–10 weeks of age. All protocols were reviewed by the Albany Medical College Ethics Committee utilizing NIH standards.

Inactivation and Labeling of *Ft*

Inactivated *Ft* (i*Ft*) was generated by growing GFP-expressing *Ft* LVS in MHB medium (BD Biosciences) up to a density of 1×10^9 CFU/ml. The culture was then spun down at 22,000g for 20 minutes at 4°C, and washed 3 times with PBS, resuspended in 2% paraformaldehyde (Sigma) and incubated 2 hours at room temperature on a rocker. Bacteria were then washed 3 more times with PBS and 1×10^9 organisms were plated on a chocolate agar plate (BD Biosciences) to confirm inactivation. The plate was then incubated for 7 days at 37°C. HEL labeling of i*Ft* was done by using a Rapid Conjugation Kit (AbD Serotec, Raleigh, NC). Briefly, 1×10^{10} i*Ft* organisms were resuspended in 200 μl of PBS and 20 μl of modifier reagent (provided with the kit) along with 500 to 1000 μg of HEL dissolved in PBS. This mixture was then incubated at room temperature overnight. The following day 20 μl of quencher (provided with the kit) were added to the i*Ft* organisms and this was incubated for 30 minutes at room temperature. Then the labeled i*Ft* was washed with PBS 2 times. The final concentration of i*Ft* organisms was determined by OD at 610 nm, HEL labeling was verified by ELISA and anti-i*Ft* mAb binding to the HEL-labeled i*Ft* was verified by flow cytometry and ELISA.

Generation of mAb + i*Ft* ICs

To generate mAb + i*Ft* ICs, 1×10^9 i*Ft* LVS organisms were incubated at 4°C overnight on a rocker with 0, 1, or 5 μg/ml of IgG2a anti-i*Ft* LPS mAb in PBS. Following the incubation, i*Ft* or mAb + i*Ft* ICs were administered to mice i.n.

SDS-PAGE and Western Blot Analysis

The IgG2a anti-*Ft* LPS mAb and i*Ft* were incubated as previously indicated [2] and as briefly described above. To avoid detection of free mAb by the goat anti-mouse mAb used to detect

ICs, following the incubation of mAb + i*Ft* ICs, free/unbound mAb was removed via centrifugation. Samples of i*Ft* [10μg (~1×10^8 organisms of i*Ft* or mAb-i*Ft* ICs)] were mixed with Laemelli sample buffer and boiled for 10 minutes prior to resolution through 4–12 % gradient SDS-PAGE pre-cast gels (Invitrogen). The running buffer was NuPAGE MES SDS buffer from Invitrogen; gels were run at 120 Volts. Resolved samples were transferred to nitrocellulose membranes. Membranes were blocked for 1 hour with PBS, 0.05% Tween 20, 2.5% horse serum and 1% casein. Biotinylated goat anti-mouse Ig heavy (γ) chain from Southern Biotech (Birmingham, AL) was used as the primary Ab for overnight incubations at a dilution of 1:1,000 in blocking buffer; streptavidin-conjugated HRP at a dilution of 1:5000 for 1 hr was used for detection. Development of the chemiluminescent substrate (SuperSignal West Pico, Pierce, Rockford, IL) was visualized using an Alpha Innotech imaging system in movie mode. Densitometric analysis of developed blots was performed on the same system. Following development of the Ig heavy chain (HC) signals, we re-probed the membranes for total *FopA* (a constitutively-expressed *Francisella* protein) and quantified the data as surface mAb/total *FopA*. These ratios were normalized to the corresponding ratios from mAb-i*Ft* -1 μg of mAb.

Immunization and Challenge Studies

C57BL/6 mice were immunized on days 0 and 21 (*Ft* LVS challenge) or days 0, 14 and 28 (*Ft* SchuS4 challenge) with 2×10^7 i*Ft* organisms alone or in the form of mAb + i*Ft* ICs utilizing IgG2a anti-i*Ft* LPS mAb. On day 35 (*Ft* LVS) or day 42 (*Ft* SchuS4) the mice were challenged with 20,000 CFU of live *Ft* LVS or 21 CFU of live *Ft* SchuS4. Following challenge survival was monitored for 21 days.

Ag Presentation Assays

APCs (2×10^5) from Balb/c mice and the *Ft*-specific T cell hybridoma cells (FT25 6D10) (1×10^5) were added in T cell medium to the wells of a 96-well plate containing i*Ft* alone or i*Ft* pre incubated 2 hours at 37°C with whole anti-i*Ft* mAb (1 μg/ml), an F(ab′)$_2$ anti-i*Ft* mAb, or an IgG2a isotype control Ab. The plate was then incubated at 37°C in 5% CO$_2$ in a humidity chamber for 24 hours and supernatants were collected. The supernatants were then assayed for IL-5 using BD Biosciences Cytometric Bead Array (CBA) following vendor instructions. In the case of Ag presentation assays specific for HEL, APCs (2×10^5) from C3H/HeN mice and the HEL-specific T cell hybridoma cells (LY50.5) (1×10^5) were added in T cell medium to the wells of a 96-well plate containing endotoxin free HEL and i*Ft* alone or i*Ft* pre-incubated with 1 μg/ml of anti-i*Ft* mAb. Alternatively, HEL-conjugated i*Ft* alone or pre-incubated with 1 μg/ml of anti-i*Ft* mAb was added to the wells. The plates were then incubated and supernatants harvested and analyzed as indicated above.

Monitoring Ag Presentation Kinetics/Persistence

Three approaches were used to measure persistence of Ag presentation. In the first instance, APCs (2×10^5) were cultured in the presence of (1×10^6) i*Ft* organisms alone or with 1 μg/ml of anti-i*Ft* mAb for either 0, 1, 2, 4, 8, 22, or 26 hours at 37C in 5% CO2. At each specified time point, the APCs were fixed with 1% paraformaldehyde (Sigma), washed 3 times with media and maintained at 4°C until the end of the time course. Once the final time point was

reached and all APCs were fixed, they were recounted and 2×10^5 APCs were added to the wells of a 96 well plate containing 1×10^5 *Ft*-specific T cell hybridoma cells. Supernatants were collected 24 hours later and IL-5 was measured using CBA. <u>In the second instance,</u> APCs (2×10^5) were cultured in the presence of (1×10^6) i*Ft* organisms alone or with 1 μg/ml of anti-i*Ft* mAb for 8 hours at 37°C in 5% CO2. Following the incubation, the APCs were washed 3 times with media and incubated at 37°C for another 0, 15, 18, 21, or 36 hours, fixed with 1% paraformaldehyde (Sigma), washed 3 times with media and kept at 4°C until the end of the time course. Once the last time point was reached and all APCs were fixed, they were re-counted and 2×10^5 APCs were added to the wells of a 96 well plate containing 1×10^5 *Ft*-specific T cell hybridoma cells. Supernatant were then collected 24 hours later and IL-5 was measured as described above. <u>In the third instance,</u> APCs (2×10^6) were cultured in the presence of (5×10^6) i*Ft* organisms alone or with 1 μg/ml of anti-i*Ft* mAb for 12 hours at 37°C in 5% CO2. Then, the APCs were washed 3 times with media and seeded on the wells of a 96 well plate containing the *Ft*-specific T cell hybridoma cells (1:1 ratio). Each day for the following 4 days supernatants were collected and the wells were replenished with fresh media. IL-5 was measured as described above. In some instances data was normalized using percent maximal response to facilitate comparisons between figures or to combine data from multiple experiments into a single figure. This was done by taking cytokine values for individual samples and dividing by the maximal cytokine value obtained for the experiment. These values were then multiplied by 100 in order to calculate percent maximal response.

i*Ft* Binding Studies

Binding of i*Ft* to APCs in the presence and absence of anti-i*Ft*-specific mAb, was visualized by flow cytometry. Experiments were carried out at 4°C to prevent i*Ft* internalization. Briefly, 2×10^5 APCs were added to the wells of a 96-well plate. Cells were washed two times with PBS containing 2mg/ml BSA and 0.1% azide, and then 100 μl of PBS-BSA-azide containing i*Ft* alone or i*Ft* plus 1 μg/ml of anti-i*Ft* mAb was added to the wells. The plate was then incubated for 2 hours at 4°C on a rocker, the cells were then washed with PBS-BSA-azide 3 times, fixed with 2% paraformaldehyde and subsequently analyzed on either a FACSCanto or LSRII flow cytometer (BD Biosciences). Alternatively, to demonstrate FcR specificity of the observed binding, the APCs were pre-incubated with non-specific monomeric mouse IgG2a (blocks FcγRI), F(ab′)$_2$ anti-mouse CD16/32 (2.4G2) (blocks FcγRII and FcγRIII), or both IgG2a and F(ab′)$_2$ 2.4G2 mAb, for 90 minutes on ice prior to adding i*Ft* plus or minus anti-i*Ft* mAb. To visualize i*Ft* binding using fluorescence microscopy, after the 2 hour incubation and subsequent washes, the cells were resuspended in PBS-azide containing Cholera Toxin subunit B-Alexa Fluor 647 conjugate (5ug/ml), which labels cell membranes, incubated for 15 minutes at 4°C and then fixed. After fixation cells were attached to a coverslip previously coated with CellTak (BD Biosciences) and mounted on a slide. Observation and image acquisition was done using an Olympus IX 81 confocal microscope (Olympus America Corporation, Center Valley, CA).

Internalization Studies

Internalization of i*Ft* in the presence and absence of anti-i*Ft* mAb was visualized by flow cytometry. Briefly, APCs (2×10^5) were pulsed with 200 to 2000 i*Ft* organisms/APC plus and minus 1 μg/ml anti-i*Ft* mAb for 1 hour at 4°C in HEPES-RPMI-10% FBS. After the

pulse, the cells were washed 3 times with 250μl of cold HEPES-RPMI, resuspended in culture media, and incubated at 37°C for the desired time. Once the incubation was complete, the cell suspension was cooled immediately on ice and washed 2 times with PBS BSA 0.1% azide. The cells were then resuspended in 100 μl of 400 μg/ml pronase [in PBS plus 0.1% azide (Prevents further i*Ft* internalization)] and subsequently incubated at 37°C for 15 minutes to strip from the cell surface the non-internalized i*Ft*. After Pronase treatment, the cells were washed and fixed with 2% paraformaldehyde. The samples were analyzed on a FACSCanto flow cytometer (BD Biosciences).

Surface Marker Expression by APCs

APCs (2×10^5) were added to the wells of a non-binding surface 96 well plate and incubated at 37°C in 5% CO_2 in the presence of i*Ft* alone or anti-i*Ft* mAb + i*Ft* ICs. After 24 hours the cells were washed 3 times with PBS-BSA-azide, resuspended in blocking buffer [PBS-BSA-azide plus 30 μg/ml of normal mouse IgG (Sigma)] and incubated on ice for 30 minutes. Cells were then washed 3 times with PBS-BSA-azide and fluorescently labeled Ab to MHC class II, F4/80, CD80, CD83, DEC205 or CD86 or their corresponding isotype controls were added. The cells were then incubated on ice for 30 minutes, washed, and then fixed with 2% paraformaldehyde. Cells were then analyzed by flow cytometry on an LSRII flow cytometer (BD Biosciences).

In Vivo Trafficking of i*Ft* and i*Ft* in mAb + i*Ft* ICs

Wildtype C57BL/6 mice or FcRn deficient mice on the same genetic background, were immunized i.n. with either i*Ft* (2×10^7 organisms/mouse) or anti-i*Ft* mAb + i*Ft* ICs at a mAb concentration of 1 μg/ml. At 30 minute intervals for a period of 3 hours, a single mouse from each group was euthanized, and the NALT was harvested. To detect the trafficking of i*Ft*, total *Ft* genomic DNA was isolated from the NALT samples using the DNeasy Blood and Tissue kit (Qiagen, Valencia, CA). A BioRad iQ5 Multicolor Real-Time PCR Detection System (Hercules, CA) was used to amplify and detect the *Francisella* gene, *fopA,* as an indication of i*Ft* trafficking to the NALT. The amount of target *Francisella* DNA was determined based upon calculations using standard curves established with plasmids containing the cloned fragment of the *Ft fopA* gene. More specifically, total *Ft* genomic DNA was obtained by using the DNeasy Blood and Tissue kit, and the 600 bp *fopA* gene was amplified by PCR. Both the forward (ACTTATAGCGCTTTGACTAACAAGGAC) and reverse (CTGCTGGTATTAAGCAATGTGAAGGC) primers were designed and purchased by Integrated DNA Technologies (Coralville, IA). The desired PCR product (tac ttatagcgct ttgactaaca aggacaatac ttggggtcct caagatagaa ctggccagtg gtacttaggt gtagatgcta acggtctagc tggaactcct aactctccat caggtgctgg tgctaacttc acaatcggtt ataacatcaa taaatacttc gctgtacagt acaaccaatt agttggtaga gtatttgctg gtttaggtga aggtgttgta aactttagta ataatactat gtttactcca tatgctgcag gtggtgctgg ttgggcaaat ctagcaggtc aagcaacagg tgcttgggat gtgggtggtg gtcttaagtt tgaactatct agaaatgttc aagcaagtgt tgactacaga tatatccaaa caatggcacc tagtaatatt tctggtgcta atggcagagc gggtactaac atgattggtg ctggttttaac atggttcttt ggtggcaaag atactactaa taatgacact ggtaatattc aggataatgg tgcgactaca gctgctcaaa ctgttgctat gccaactatt gatgagtcta gtatgttttt acctgctggt attaagcaat gtgaaggc) was gel purified and cloned in pCR4-TOPO plasmid vector (Invitrogen, Carlsbad, CA), and was subsequently used to transform chemically competent

DH5a *E. coli* cells. Kanamycin resistant *E. coli* colonies were selected and the plasmid DNA was isolated, sequenced, and used as a real-time PCR standard. The numbers of *fopA* copies from each sample were normalized against 10,000 copies of the mouse gene *Nidogen.*

Statistical Analysis

The Log-Rank (Mantel-Cox) test was used for survival curves. One-way analysis of variances (ANOVA) or the unpaired, one-tailed student t-test was used for the remaining figures. GraphPad Prism 4 provided the software for the statistical analysis (San Diego, CA).

Acknowledgments

References

1. McLendon MK, Apicella MA, Allen LA. Francisella tularensis: taxonomy, genetics, and Immunopathogenesis of a potential agent of biowarfare. Annu Rev Microbiol. 2006; 60:167–85. [PubMed: 16704343]

2. Rawool DB, Bitsaktsis C, Li Y, Gosselin DR, Lin Y, Kurkure NV, et al. Utilization of Fc receptors as a mucosal vaccine strategy against an intracellular bacterium, Francisella tularensis. J Immunol. 2008; 180:5548–57. [PubMed: 18390739]

3. McGhee JR. A mucosal gateway for vaccines. Nat Biotechnol. 2011; 29:136–8. [PubMed: 21301439]

4. Lu L, Palaniyandi S, Zeng R, Bai Y, Liu X, Wang Y, et al. A neonatal Fc receptor-targeted mucosal vaccine strategy effectively induces HIV-1 antigen-specific immunity to genital infection. J Virol. 2011; 85:10542–53. [PubMed: 21849464]

5. Ye L, Zeng R, Bai Y, Roopenian DC, Zhu X. Efficient mucosal vaccination mediated by the neonatal Fc receptor. Nat Biotechnol. 2011; 29:158–63. [PubMed: 21240266]

6. Bitsaktsis C, Iglesias BV, Li Y, Colino J, Snapper CM, Hollingshead SK, et al. Mucosal immunization with an unadjuvanted vaccine that targets Streptococcus pneumoniae PspA to human Fcgamma receptor type I protects against pneumococcal infection through complement-and lactoferrin-mediated bactericidal activity. Infect Immun. 2012; 80:1166–80. [PubMed: 22158740]

7. Amigorena S, Bonnerot C. Fc receptors for IgG and antigen presentation on MHC class I and class II molecules. Semin Immunol. 1999; 11:385–90. [PubMed: 10625592]

8. Gosselin EJ, Bitsaktsis C, Li Y, Iglesias BV. Fc receptor-targeted mucosal vaccination as a novel strategy for the generation of enhanced immunity against mucosal and non-mucosal pathogens. Arch Immunol Ther Exp (Warsz). 2009; 57:311–23. [PubMed: 19688186]

9. Heyman B. Regulation of antibody responses via antibodies, complement, and Fc receptors. Annu Rev Immunol. 2000; 18:709–37. [PubMed: 10837073]

10. van der Poel CE, Spaapen RM, van de Winkel JG, Leusen JH. Functional characteristics of the high affinity IgG receptor, FcgammaRI. J Immunol. 2011; 186:2699–704. [PubMed: 21325219]

11. Jelley-Gibbs DM, Plitnick LM, Gosselin EJ. Differences in IgG subclass do not effect immune complex-enhanced T cell activation despite differential binding to antigen presenting cells. Hum Immunol. 1999; 60:469–78. [PubMed: 10408796]

12. Boruchov AM, Heller G, Veri MC, Bonvini E, Ravetch JV, Young JW. Activating and inhibitory IgG Fc receptors on human DCs mediate opposing functions. J Clin Invest. 2005; 115:2914–23. [PubMed: 16167082]

13. Laborde EA, Vanzulli S, Beigier-Bompadre M, Isturiz MA, Ruggiero RA, Fourcade MG, et al. Immune complexes inhibit differentiation, maturation, and function of human monocyte-derived dendritic cells. J Immunol. 2007; 179:673–81. [PubMed: 17579090]

14. Guyre CA, Keler T, Swink SL, Vitale LA, Graziano RF, Fanger MW. Receptor modulation by Fc gamma RI-specific fusion proteins is dependent on receptor number and modified by IgG. J Immunol. 2001; 167:6303–11. [PubMed: 11714794]

15. Fridman WH. Regulation of B-cell activation and antigen presentation by Fc receptors. Curr Opin Immunol. 1993; 5:355–60. [PubMed: 8347298]

16. Guriec N, Daniel C, Le Ster K, Hardy E, Berthou C. Cytokine-regulated expression and inhibitory function of FcgammaRIIB1 and -B2 receptors in human dendritic cells. J Leukoc Biol. 2006; 79:59–70. [PubMed: 16244114]

17. Nimmerjahn F, Ravetch JV. Fc-receptors as regulators of immunity. Adv Immunol. 2007; 96:179–204. [PubMed: 17981207]

18. Bayry J, Lacroix-Desmazes S, Kazatchkine MD, Hermine O, Tough DF, Kaveri SV. Modulation of dendritic cell maturation and function by B lymphocytes. J Immunol. 2005; 175:15–20. [PubMed: 15972625]

19. Gondre-Lewis TA, Moquin AE, Drake JR. Prolonged antigen persistence within nonterminal late endocytic compartments of antigen-specific B lymphocytes. J Immunol. 2001; 166:6657–64. [PubMed: 11359820]

20. Bitonti AJ, Dumont JA, Low SC, Peters RT, Kropp KE, Palombella VJ, et al. Pulmonary delivery of an erythropoietin Fc fusion protein in non-human primates through an immunoglobulin transport pathway. Proc Natl Acad Sci U S A. 2004; 101:9763–8. [PubMed: 15210944]

21. Liu X, Lu L, Yang Z, Palaniyandi S, Zeng R, Gao LY, et al. The neonatal FcR-mediated presentation of immune-complexed antigen is associated with endosomal and phagosomal pH and antigen stability in macrophages and dendritic cells. J Immunol. 2011; 186:4674–86. [PubMed: 21402891]

22. Spiekermann GM, Finn PW, Ward ES, Dumont J, Dickinson BL, Blumberg RS, et al. Receptor-mediated immunoglobulin G transport across mucosal barriers in adult life: functional expression of FcRn in the mammalian lung. J Exp Med. 2002; 196:303–10. [PubMed: 12163559]

23. Yoshida M, Claypool SM, Wagner JS, Mizoguchi E, Mizoguchi A, Roopenian DC, et al. Human neonatal Fc receptor mediates transport of IgG into luminal secretions for delivery of antigens to mucosal dendritic cells. Immunity. 2004; 20:769–83. [PubMed: 15189741]

24. White DM, Pellett S, Jensen MA, Tepp WH, Johnson EA, Arnason BG. Rapid immune responses to a botulinum neurotoxin Hc subunit vaccine through in vivo targeting to antigen-presenting cells. Infect Immun. 2011; 79:3388–96. [PubMed: 21576339]

25. Adamova E, Walsh MC, Gosselin DR, Hale K, Preissler MT, Graziano RF, et al. Enhanced antigen-specific antibody and cytokine responses when targeting antigen to human FcGAMMA receptor type I using an anti-human FcGAMMA receptor type I-streptavidin fusion protein in an adjuvant-free system. Immunol Invest. 2005; 34:417–29. [PubMed: 16304730]

26. Gosselin EJ, Wardwell K, Gosselin DR, Alter N, Fisher JL, Guyre PM. Enhanced antigen presentation using human Fc gamma receptor (monocyte/macrophage)-specific immunogens. J Immunol. 1992; 149:3477–81. [PubMed: 1431118]

27. Guyre PM, Graziano RF, Goldstein J, Wallace PK, Morganelli PM, Wardwell K, et al. Increased potency of Fc-receptor-targeted antigens. Cancer Immunol Immunother. 1997; 45:146–8. [PubMed: 9435859]

28. Heijnen IA, van Vugt MJ, Fanger NA, Graziano RF, de Wit TP, Hofhuis FM, et al. Antigen targeting to myeloid-specific human Fc gamma RI/CD64 triggers enhanced antibody responses in transgenic mice. J Clin Invest. 1996; 97:331–8. [PubMed: 8567952]

29. Man AL, Prieto-Garcia ME, Nicoletti C. Improving M cell mediated transport across mucosal barriers: do certain bacteria hold the keys? Immunology. 2004; 113:15–22. [PubMed: 15312131]
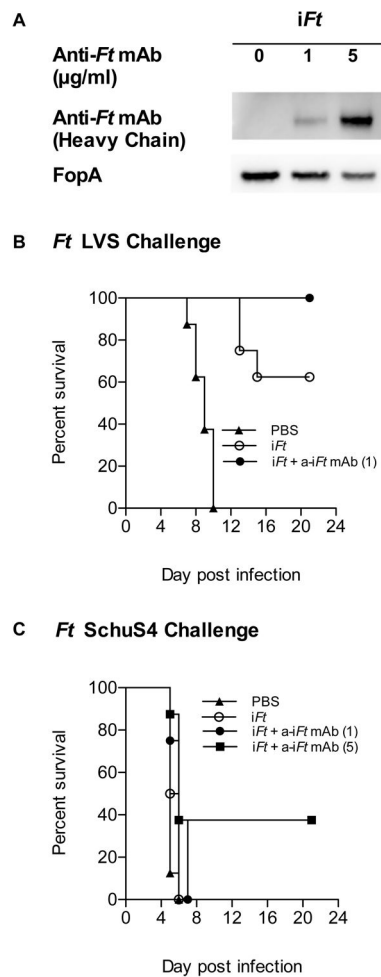
Figure 1. Enhanced protection is observed using anti-i*Ft* mAb + i*Ft* ICs

Prior to immunization, 1×10^9 i*Ft* organisms were incubated at 4°C overnight with 0, 1 or 5 μg/ml of anti-i*Ft* mAb in PBS. Following the incubation, i*Ft* and mAb + i*Ft* ICs were washed (to remove free mAb) and analyzed by SDS PAGE and Western Blot to verify mAb-i*Ft* IC formation (A). 2×10^7 i*Ft* organisms alone or complexed with anti-i*Ft* mAb were administered i.n. to C57BL/6 mice. The mice were boosted on day 21 and challenged on day 35 with either 20,000 CFU of *Ft* LVS (B) or boosted on days 14 and 28 and challenged on day 42 with 21 CFU of *Ft* SchuS4 (C). Survival was monitored for 21 days. The p value for i*Ft* versus mAb + i*Ft* ICs in B (*Ft* LVS challenge) was < 0.05. The p value for i*Ft* versus mAb + i*Ft* ICs in C (*Ft* SchuS4 challenge, 5 μg) was < 0.02.
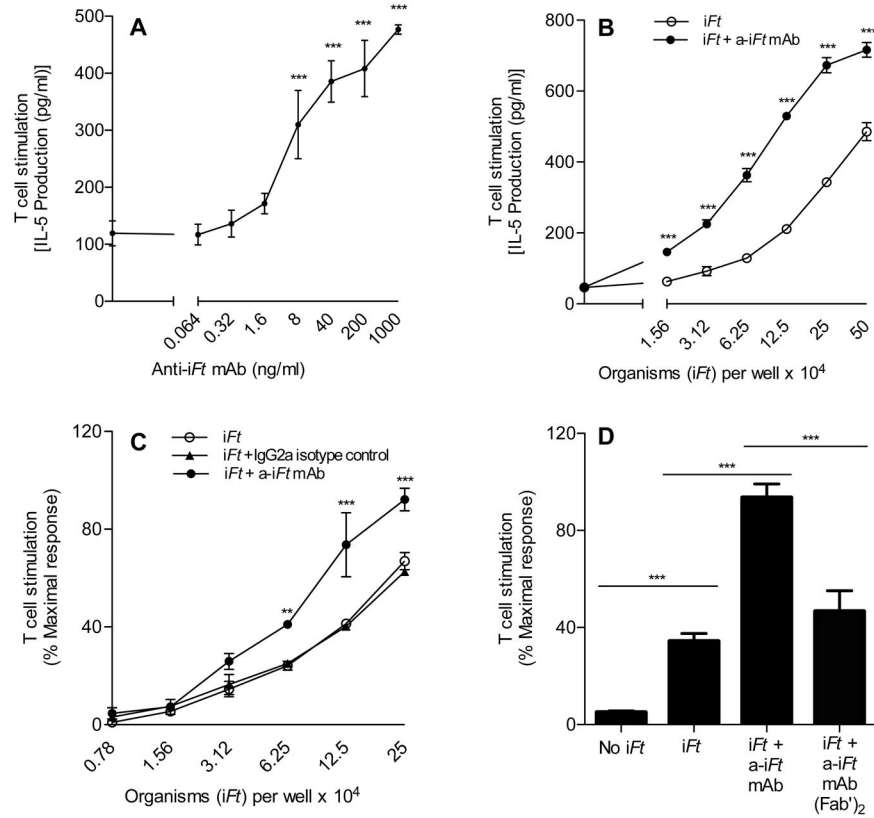
Figure 2. Presentation of i*Ft* to *Ft*-specific T cells is enhanced in the presence of anti-i*Ft* mAb
Ft-specific T cell hybridoma cells (1×10^5 cells/well) were cultured with Balb/c MØs (2×10^5 cells/well) in the presence of: increasing concentrations of anti-i*Ft* mAb and a fixed concentration of i*Ft* organisms (4×10^5 per well) (A), increasing amounts of i*Ft* organisms plus and minus 1 μg/ml of anti-i*Ft* mAb (B), increasing amounts of i*Ft* organisms either alone, plus 1 μg/ml of anti-i*Ft* mAb, or plus a non-specific IgG2a isotype control mAb (C), media, 4×10^5 i*Ft*/well, or 4×10^5 i*Ft*/well plus 0.04 μg/ml of anti-i*Ft* mAb or 0.04 μg/ml of F(ab′)$_2$ anti-i*Ft* mAb (D). Production of IL-5 by *Ft*-specific T cells was measured in all figures (A–D) as an indicator of T cell response to i*Ft* by CBA. In the case of (C) and (D) data was normalized between experiments by expressing results as percent maximal response. Results are representative of three independent experiments. (***) p value < 0.001.
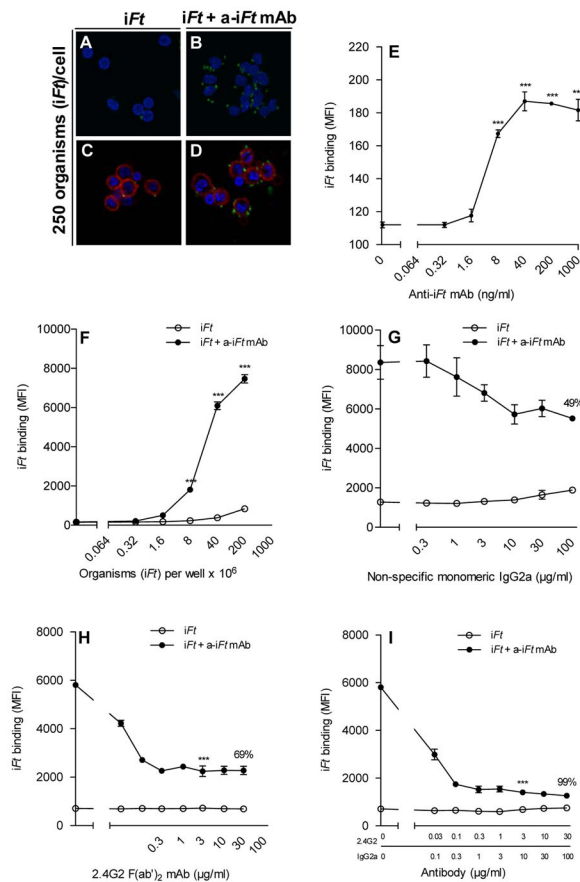
Figure 3. Anti-i*Ft* mAb enhances FcR-dependent binding of i*Ft* to APCs
Z projections of Balb/c MØs incubated for 2 hours at 4°C with either i*Ft* alone or anti-i*Ft*
mAb + i*Ft* ICs. The i*Ft* (green) (GFP expressing inactivated *Ft* organisms) can be seen on
the cells' surface (red) labeled with CTB Alexa 647 and the nuclei (blue) have been stained
with DAPI. The images were acquired on an Olympus IX 81 confocal microscope (A–D).
Balb/c MØs were incubated at 4°C for 2 hours in the presence of either increasing
concentrations of anti-i*Ft* mAb and 5×10^5 i*Ft* organisms per well (E), or increasing
concentrations of i*Ft* organisms plus or minus 1 μg/ml of anti-i*Ft* mAb (F). Prior to the
addition of the i*Ft* organisms in the presence or absence of anti-i*Ft* mAb, FcγR were blocked
for 1 hour at 4°C with monomeric IgG2a (FcγRI) (G), F(ab′)$_2$ 2.4G2 mAb (FcγRII and
FcγRIII) (H), or both IgG2a and F(ab′)$_2$ 2.4G2 mAb (I). Binding of GFP-expressing i*Ft*
organisms was detected by flow cytometry using a BD LSRII flow cytometer (E–I). Results
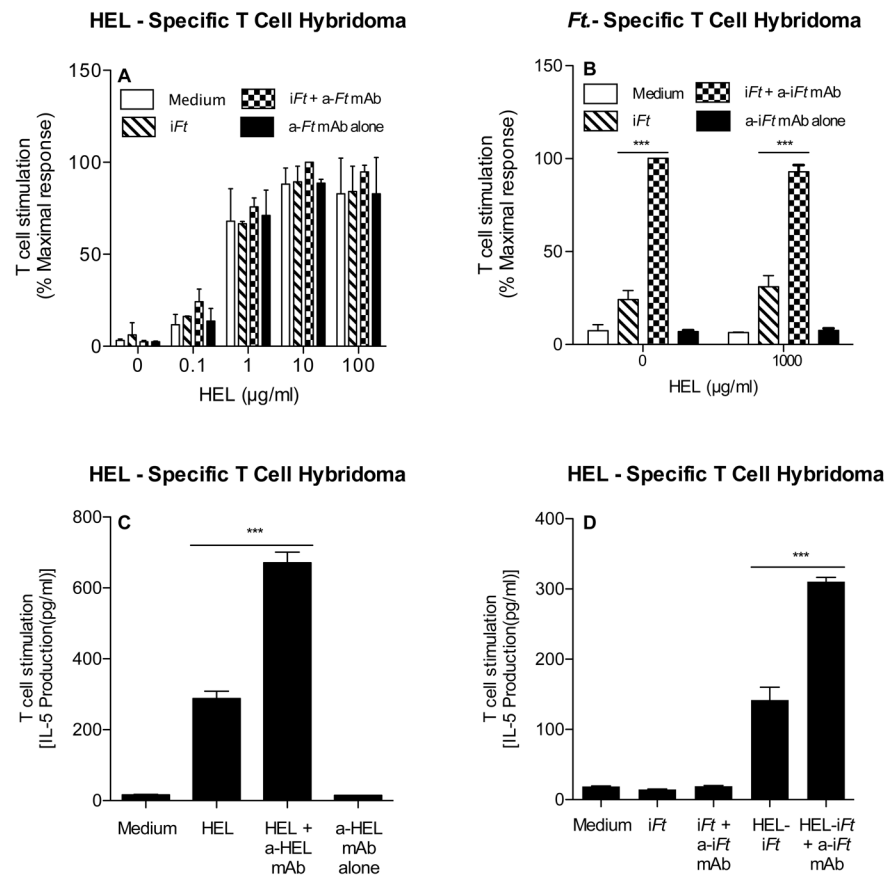are representative of three independent experiments. (***) p value < 0.001.

Figure 4. A physical linkage between mAb and Ag is required for FcR-mediated enhancement of Ag presentation by APCs

HEL-specific T cell hybridoma cells (1×10^5 cells/well) were cultured with C3H/HeN MØs (2×10^5 cells/well) in the presence of media, 5×10^5 i*Ft* organisms/well alone or plus 1μg/ml of anti-i*Ft* mAb and increasing amounts of HEL (A). *Ft*-specific T cell hybridoma cells (1×10^5 cells/well) were cultured with Balb/c MØs (2×10^5 cells/well) in the presence or absence of 1 mg/ml of HEL in media, 5×10^5 i*Ft* organisms/well alone or plus 1μg/ml of anti-i*Ft* mAb (B). HEL specific T cell hybridoma cells (1×10^5 cells/well) were cultured with C3H/HeN MØs (2×10^5 cells/well) in the presence of media, 0.1 mg/ml of HEL, 0.1 mg/ml of HEL plus anti-HEL mAb (2D1), or anti-HEL mAb alone (2D1) (C). HEL-specific T cell hybridoma cells (1×10^5 cells/well) were cultured with C3H/HeN MØs (2×10^5 cells/well) in the presence of media, 2×10^7 i*Ft* organisms plus or minus anti-i*Ft* mAb, or 2×10^7 HEL conjugated i*Ft* organisms plus or minus anti-i*Ft* mAb (D). Production of IL-5 by *Ft*-specific T cells was measured in all figures (A–D) as an indicator of T cell response to i*Ft* by CBA. Data was normalized between experiments by expressing results as percent maximal response. Results in 2A and 2B represent the combined data from two independent experiments. All other results are representative of three independent experiments. (***) p value < 0.001.
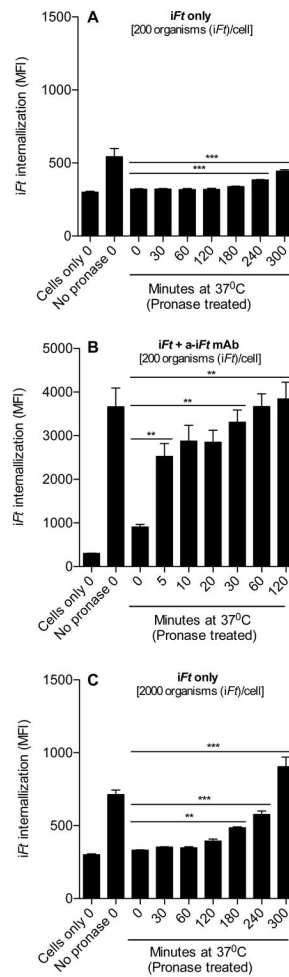
Figure 5. Internalization of i*Ft* is enhanced in the presence of anti-i*Ft* mAb
Balb/c MØs (2×10^5 cells) were pulsed with 200 i*Ft* organisms/MØ in the absence (A) or presence (B) of anti-i*Ft* mAb for 1 hour at 4°C. After the pulse, the unbound i*Ft* was removed and the MØs were incubated at 37°C to allow internalization of the i*Ft*. At the end of each 37°C incubation time point, the non-internalized i*Ft* was stripped from the cell surface using pronase, and the amount of internalized i*Ft* was measured by flow cytometry (A–B). In addition, MØs were also pulsed with 2000 i*Ft* organisms/MØ in the absence of anti-i*Ft* mAb. The experiment was then carried out as in A and B. Internalization is reflected as increased MFI following incubation and pronase treatment, as compared to pronase-treated cells at time zero. Results are representative of three independent experiments. (**) p value < 0.01, (***) p value < 0.001.
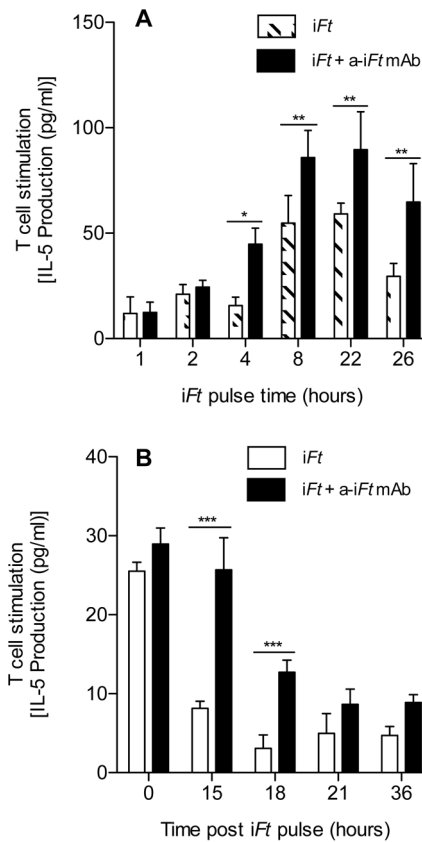
Figure 6. Enhanced presentation of i*Ft* persists in the presence of anti-i*Ft* mAb
Balb/c MØs (2×10^5 cells) were cultured in media alone or media containing 1×10^6 i*Ft* organisms in the presence or absence of 1 μg/ml of anti-i*Ft* mAb at 37°C in 5% CO_2 for 0, 1, 2, 4, 8, 22 or 26 hours. At each time point the cells were then fixed for 15 minutes at room temperature in 1% paraformaldehyde, washed, and stored at 4°C until all time points were completed. Cells were then counted and adjusted to 2×10^6 cells/ml, 100 μl of the latter were then added to the wells of a 96 well plate containing the *Ft*-specific T cell hybridoma at 1×10^5 cells/well. The plate was then incubated at 37°C in 5% CO_2 in a humidity chamber for 24 hours, the supernatant was collected, and assayed for IL-5 using CBA. The average of three independent experiments is presented (A). Balb/c MØs (2×10^5 cells) were cultured in media alone or media containing 1×10^6 i*Ft* organisms in the presence or absence of 1 μg/ml of anti-i*Ft* mAb for 8 hours at 37°C in 5% CO_2. After the incubation, the cells were washed 3 times with PBS and further incubated at 37°C in 5% CO_2 for 0, 15, 18, 21 or 36 hours, at which point they were fixed with 1% paraformaldehyde, washed with PBS and then stored at 4°C until all time points were completed. Subsequently, cells were counted and adjusted to 2×10^6 cells/ml and 100 μl of the latter were then added to the wells of a 96 well plate containing the *Ft*-specific T cell hybridoma at 1×10^5 cells/well. The plate was incubated at 37°C in 5% CO_2 in a humidity chamber for 24 hours and the supernatant was collected. The supernatants were assayed for IL-5 using CBA (B). Results are representative of three independent experiments. (*) p value < 0.05, (**) p value < 0.01, (***) p value < 0.001.
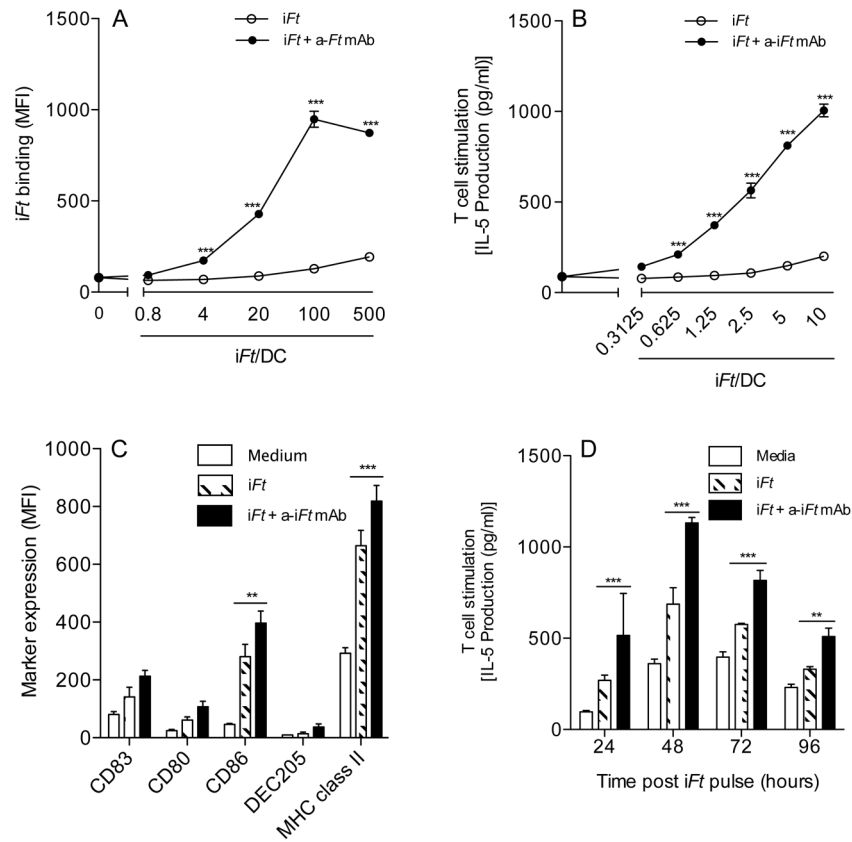
Figure 7. Enhanced i*Ft* binding, presentation, and persistence are also observed when using DCs as APCs

Balb/c bone marrow-derived DCs were incubated for 2 hours at 4°C in the presence of increasing concentrations of i*Ft* organisms plus or minus 1μg/ml of anti-i*Ft* mAb. Binding of GFP-expressing i*Ft* organisms to DCs was detected by flow cytometry using a BD LSRII flow cytometer (A). *Ft*-specific T cell hybridoma cells were cultured with Balb/c bone marrow-derived DCs in the presence of increasing concentrations of i*Ft* organisms in the presence or absence of 1 μg/ml of anti-i*Ft* mAb (B). Balb/c bone marrow-derived DCs (5×10^5) were cultured for 24 hours at 37°C in 5% CO_2 in the presence of media alone or 1×10^7 i*Ft* organisms plus or minus 1 μg/ml of anti-i*Ft* mAb. Following the incubation, cells were washed PBS/BSA and stained for CD83, CD80, CD86, DEC205, and MHC class II. Fluorescence was detected by flow cytometry on a LSRII flow cytometer (C). Balb/c bone marrow-derived DCs were pulsed for 12 hours at 37°C in 5% CO_2 with media alone, i*Ft* organisms (MOI 2.5), or i*Ft* organisms plus 1 μg/ml of anti-i*Ft* mAb. After the pulse, the DCs were washed three times with media and incubated with the *Ft*-specific T cell hybridoma cells (2:1 ratio) at 37°C in 5% CO_2. Every 24 hours the media from each well was collected and stored at −20°C. Fresh media was added to the wells each day after collecting the sample. This was done for 4 days. Production of IL-5 by *Ft*-specific T cells was measured as an indicator of T cell response to i*Ft* by CBA and normalized between experiments by expressing results as percent maximal response (D). Results are representative of three independent experiments. (**) p value < 0.01, (***) p value < 0.001.
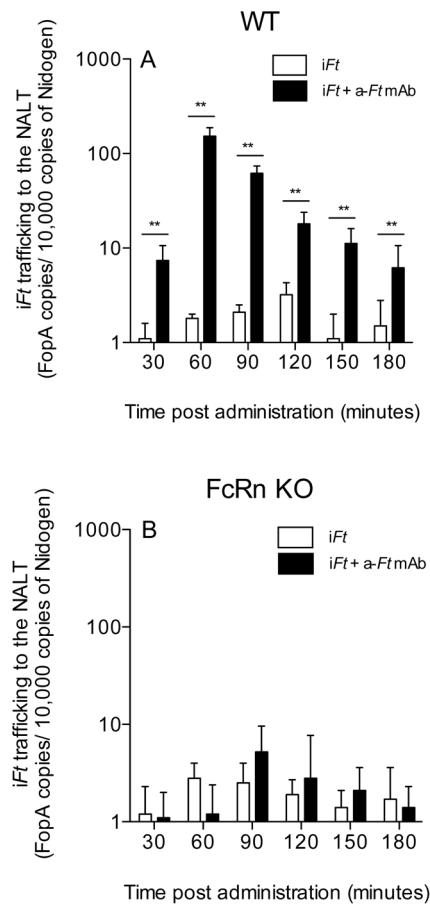
Figure 8. Trafficking of i*Ft* to the NALT is enhanced and is FcRn-dependent in the presence of anti-i*Ft* mAb

C57BL/6 (A) or FcRn deficient (B) mice were immunized i.n. with either i*Ft* (2×10^7 CFUs/mouse) plus or minus anti-i*Ft* mAb (1ug/ml). At 30 minute intervals the NALT from a single mouse from each group was harvested. Genomic DNA was isolated and the number of *FopA* gene copies present was determined by multiplex real-time PCR. Equal amounts of total chromosomal DNA were added to each reaction (50 ng/reaction). Each sample was run in triplicate and the results were then normalized against 10,000 copies of the mouse gene, Nidogen. Data in A is representative of three independent experiments. (**) p value < 0.01.